

Solar thermal energy application to dry reforming of methane on the open-cell foam to enhance the energy storage efficiency of a thermochemical fluidized bed membrane reformer: modelling and simulation

Aplicação de energia térmica solar para reforma a seco de metano na espuma de células abertas para aumentar a eficiência de armazenamento de energia de um reformador de membrana de leito fluidizado termoquímico: modelagem e simulação

Aplicación de energía solar térmica para el reformado en seco de metano en la espuma de celda abierta para mejorar la eficiencia de almacenamiento de energía de un reformador de membrana de lecho fluidizada termoquímico: modelado y simulación

Received: 11/24/2021 | Reviewed: 11/30/2021 | Accept: 12/05/2021 | Published: 12/16/2021

Paulo Wendel Corderceira Costa

ORCID: <https://orcid.org/0000-0002-4275-050X>

University of Pernambuco, Brazil

E-mail: paulowendel@outlook.com

Jornandes Dias da Silva

ORCID: <https://orcid.org/0000-0002-6346-1192>

University of Pernambuco, Brazil

E-mail: jornandesdias@poli.br

Abstract

The hydrodynamic characterization of the solar-driven CO₂ reforming of methane through β-SiC open-cell foam in a fluidized bed configuration is performed by reacting Methane (CH₄) with carbon dioxide (CO₂). The mathematical modelling is important to design and optimize the reforming methods. Usually, the reforming methods's application through β-SiC foam bed improves the heat transfer and mass transfer due to high porosity and surface area of the β-SiC foam. Fluidized Bed Membrane (FBM) Reformers can be substantially studied as a promising equipment to investigate the thermochemical conversion of CH₄ using CO₂ to produce solar hydrogen. This work has as main objective a theoretical modelling to describe the process variables of the solar-driven CO₂ reforming of methane in the FBM reformer. The FBM reformer is filled with β-SiC open-cell foam where the thermochemical conversion is carried out. The model variables describe the specific aims of work and these objectives can be identified from each equation of the developed mathematical model. The present work has been proposed to study two specific aims as (i) The effective thermal conductivity's effect of the solid phase and (ii) molar flows of chemical components. The endothermic reaction temperature's profiles are notably increased as the numeral value of the effective thermal conductivity's effect of the solid phase, is risen. The solar-driven CO₂ reforming method is suggested to improve the Production Rate (PR) of H₂ regarding the PR of CO.

Keywords: Open-cell; Fluidized bed; Dry reforming; Membrane reformer.

Resumo

A caracterização hidrodinâmica da reforma de CO₂ movida a energia solar de metano por meio de espuma de células abertas de β-SiC em uma configuração de leito fluidizado é realizada pela reação de metano (CH₄) com dióxido de carbono (CO₂). A modelagem matemática é importante para projetar e otimizar os métodos de reforma. Normalmente, a aplicação dos métodos de reforma através do leito de espuma de β-SiC melhora a transferência de calor e a transferência de massa devido à alta porosidade e área de superfície da espuma de β-SiC. Reformadores de membrana de leito fluidizado (RMLF) podem ser substancialmente estudados como um equipamento promissor para investigar a conversão termoquímica de CH₄ usando CO₂ para produzir hidrogênio solar. Este trabalho tem como objetivo principal uma modelagem teórica para descrever as variáveis do processo da reforma de CO₂ por energia solar do metano no reformador FBM. O reformador FBM é preenchido com espuma de células abertas β-SiC onde a conversão termoquímica é realizada. As variáveis do modelo descrevem os objetivos específicos do trabalho e esses objetivos podem ser identificados a partir de cada equação do modelo matemático desenvolvido. O presente trabalho tem como objetivo estudar dois objetivos específicos como (i) o efeito da condutividade térmica efetiva da fase sólida e (ii) fluxos molares de componentes químicos. Os perfis de temperatura da reação endotérmica são aumentados

notavelmente quando o valor numérico da condutividade térmica efetiva da fase sólida é aumentado. O método de reforma de CO₂ movido à energia solar é sugerido para melhorar a Taxa de Produção (PR) de H₂ em relação ao PR de CO.

Palavras-chave: Célula aberta; Leito fluidizado; Reforma seca; Reformador de membrana.

Resumen

La caracterización hidrodinámica del reformado de metano con CO₂ impulsado por energía solar a través de una espuma de celda abierta de β -SiC en una configuración de lecho fluidizada se realiza haciendo reaccionar metano (CH₄) con dióxido de carbono (CO₂). El modelado físico-matemático es importante para diseñar y optimizar los métodos de reforma. Por lo general, la aplicación de los métodos de reformado a través del lecho de espuma de β -SiC mejora la transferencia de calor y la transferencia de masa debido a la alta porosidad y área superficial de la espuma de β -SiC. Los reformadores de membrana de lecho fluidizada (FBM) pueden estudiarse sustancialmente como un equipo prometedor para investigar la conversión termoquímica de CH₄ utilizando CO₂ para producir hidrógeno solar. Este trabajo tiene como objetivo principal un modelado teórico para describir las variables de proceso del reformado de metano con CO₂ impulsado por energía solar en el reformador FBM. El reformador FBM se llena con espuma de celda abierta de β -SiC donde se lleva a cabo la conversión termoquímica. Las variables del modelo describen los objetivos específicos del trabajo y estos objetivos se pueden identificar a partir de cada ecuación del modelo matemático desarrollado. El presente trabajo se ha propuesto estudiar dos objetivos específicos como (i) El efecto de la conductividad térmica efectiva de la fase sólida y (ii) los flujos molares de los componentes químicos. Los perfiles de la temperatura de reacción endotérmica aumentan notablemente como valor numérico del efecto de la conductividad térmica efectiva de la fase sólida se levanta. Se sugiere el método de reformado de CO₂ impulsado por energía solar para mejorar la Tasa de Producción (PR) de H₂ con respecto a la PR de CO.

Palabras clave: Célula abierta; Lecho fluidizada; Reforma seca; Reformador de membranas.

1. Introduction

Reforming processes which make use of solar energy to drive high temperature endothermic chemical reactions are known as solar thermochemical systems. Solar catalytic reforming of carbon dioxide (CO₂) can be carried out in a Solar Fluidized Bed Membrane (SFBM) reformer as an intensification process. The intensification strategy can lead to the development and the re-design of more compact and efficient new processes that allow better exploitation of raw materials, lower energy consumption and plant volume reduction. The technology of the solar reforming process in a SFBM reformer contributes to the key innovative element of sustainable development (Villafán-Vidales et al., 2017). In dry reforming process, methane (CH₄) reacts with carbon monoxide (CO) in the reaction zone (shell) of the SFBM reformer to produce a product mixture of hydrogen (H₂) and carbon monoxide (CO) (Chein et al., 2017; Chen et al., 2018). Reforming reactions are highly endothermic and can be performed with active catalysts (Ni, Rh) at high temperature, high pressure and steam-carbon ratio (S/C) varying between 1.4 and 4 (Cruz & Silva, 2017).

Solar thermochemical reforming is based in the use of concentrated solar energy as a heating source of high temperature for conducting an endothermic chemical transformation. The solar reforming technology can be used to produce renewable energies (as solar hydrogen (H₂) production) as from solar thermochemical reaction systems (STRSs). The production of solar H₂ in SFBM reformer is highlighted by changing the reaction equilibrium toward the product side through effective pressure difference induced by the continuous removal of H₂ over the membrane (Jin et al., 2018; Reis et al., 2018). The commercial separation of H₂ through metallic membranes is mainly focused on palladium alloys membrane. Pd-based membranes have been proposed for the separation of H₂ for many years due to the selectivity to hydrogen permeation (Silva and Abreu, 2016). The fabrication of Pd membranes for the separation of H₂ has increased due the need of use in the reforming processes at high temperature, and applications for the separation processes in chemical, petrochemical, and petroleum industries.

Mathematical modelling is useful to investigate the effects of key operating parameters, optimization, and scale-up. For SFBM reformers, the permeation rate's importance on the diffusion rate needs to be included to account for radial gradients because of the polarization's effect in the vicinity of the membrane (Cruz & Silva, 2017). From the point of theoretical view,

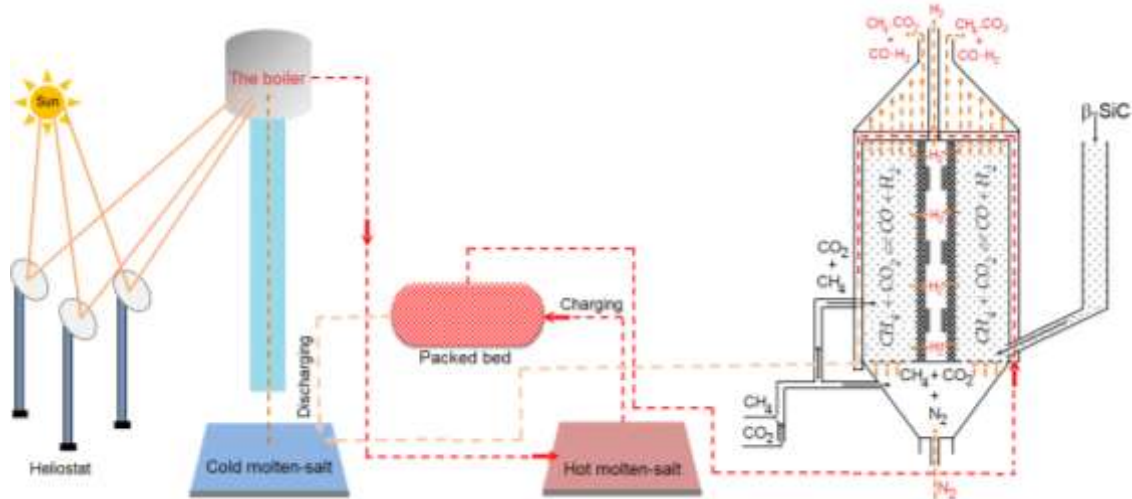
the polarization exists in all membrane separation processes due to the selective permeability of membrane (Nagy, 2010). The two-dimensional mathematical models are commonly used to estimate the temperature and concentration polarization profiles of the membrane processes (Silva et al, 2021). For this reason, a 2D approach able to systematically take into account this phenomenon is approached in this work.

In this study, a mathematical model has been developed to investigate the heat and mass transfer phenomena coupled with thermochemical reaction kinetics in SFBM reformer module. The performance from SFBM reformer using the solar reforming process is numerically investigated in terms of the temperature profiles of the endothermic reaction. On the other hand, it was also studied the reactant and product distribution as well as conversions of CH_4 and CO_2 in SFBM reformer.

2. Problem Description

The schematic setup from Figure 1 shows a solar-driven SFBM reformer module. In this setup, a solar tower and packed bed (molten-salt) are coupled to the SFBM reformer module to keep the dynamic energy storage. The first loop in the system is a closed loop of CO_2 that is heated by a solar tower and it transports the thermal energy to the fluidized bed reformer. The hot CO_2 is circled from the packed bed (molten-salt) where a portion of CO_2 come back towards the solar tower and other part is discharged into the SFBM reformer module. The inclusion of the solar tower and packed bed (molten-salt) allows for dynamic energy storage that can be used to improve the SFBM reformer module efficiency under real operating conditions. This work focuses only on the SFBM reformer module's modelling.

Figure 1: Schematic setup of a solar-driven SFBM reformer module.



Source: Authors themselves.

2.1 Methodology

The schematic setup from Figure 1 is built of solar tower, packed bed (molten-salt), and SFBM reformer module, respectively. The methodology reported in this work consists of the following steps: (i) kinetic modelling of the solar reforming process of CO_2 , (ii) SFBM reformer module modelling, (iii) shell side's model equations on the SFBM reformer module, (iv) permeate side's model equations on the SFBM reformer module, (v) numerical solution of model equations.

2.2 Kinetic mechanism

The reforming reaction of CO_2 is essential to produce H_2 and syngas (H_2 e CO) which are highly endothermic. The

reforming process has a limited equilibrium and comprises one reforming reaction as follows.



2.3 Kinetic model

The overall rate equation of the reaction, Eq. (1), is based on the Langmuir-Hinshelwood kinetic model and it can be found in Chen et al., (2018) as follows.

$$R_{CO_2} = \frac{k_{CO_2} K_{CH_4} K_{CO_2} P_{CH_4} P_{CO_2}}{\left(1 + K_{CH_4} P_{CH_4} + K_{CO_2} P_{CO_2}\right)^2} \quad (2)$$

In Eq. (2), R_{CO_2} (kmol/kg_{cat}.h) is the kinetic rate from reforming reaction; k_{CO_2} (kmol/ kg_{cat}.h) is the kinetic rate constant from reforming reaction, K_{CH_4} is the surface adsorption equilibrium constant of CH₄, K_{CO_2} (kPa⁻¹) is the surface adsorption equilibrium constant of CO₂, P_{CH_4} (kPa) is the partial pressure of CH₄, P_{CO_2} (kPa) is the partial pressure of CO₂, respectively.

2.4 Direct modelling of the heat and mass transfer

The gas-solid contact in the fluidized bed system improves the heat and mass transfer because of the interfacial surface's effect of solid particles. The use of mathematical models can be used to predict the heat and mass physical phenomena in the fluid-solid systems. Thus, it was developed a dynamic mathematical model that involves the SFBM reformer module's heat and mass transfer equations as follows.

2.5 Heat transfer in the shell side

An energy balance equation is developed to describe the gas temperature on the SFBM reformer module shell side. The governing energy balance of the gaseous phase is built as follows.

- Energy equation for the gaseous phase in the shell side;

$$\varepsilon_b \rho_{sh,b} C_{p,sh,b} \left(\frac{\partial T_{sh,b}}{\partial t} + u_b \frac{\partial T_{sh,b}}{\partial z} \right) = \lambda_{r,eff,b} \frac{1}{r} \frac{\partial}{\partial r} \left(r \frac{\partial T_{sh,b}}{\partial r} \right) - h_{bs} A_{bs} (T_{sh,b} - T_{sh,s}) \quad (3)$$

- Initial and boundary conditions for Equation (3) are defined as;

$$T_{sh,b} \Big|_{t=0} = T_{sh,b,0}; T_{sh,b} \Big|_{z=0^+} = T_{sh,b,in.}, \frac{\partial T_{sh,b}}{\partial z} \Big|_{z=L} = 0; \frac{\partial T_{sh,b}}{\partial r} \Big|_{r=R/2} = \frac{h_{bs}}{\lambda_{r,eff,b}} [T_{sh,b} - T_{sh,s}] \quad (4)$$

$$\left(T_{sh,s} + \frac{T_{sh,m} + T_{p,m}}{2} \right), \frac{\partial T_{sh,b}}{\partial r} \Big|_{r=0} = 0$$

On the other hand, an energy balance equation is also built up to report the solid temperature along the SFBM reformer module shell side as follows.

- Energy equation for the solid phase in the shell side;

$$\rho_{sh,s} C_{p,sh,s} \frac{\partial T_{sh,s}}{\partial t} = \lambda_{r,eff,s} \frac{1}{r} \frac{\partial}{\partial r} \left(r \frac{\partial T_{sh,s}}{\partial r} \right) - \rho_{sh,s} C_{p,sh,s} u_s \frac{\partial T_{sh,s}}{\partial z} - h_{sg} \frac{6}{d_p} \frac{(1-\varepsilon_b)}{\varepsilon_b} (T_b - T_s) + \rho_s \frac{(1-\varepsilon_p)}{\varepsilon_p} \Delta H_{CO_2} \eta_{CO_2} R_{CO_2} \quad (5)$$

- Initial and boundary conditions for Equation (5) are defined as;

$$T_{sh,s} \Big|_{t=0} = T_{sh,s,0}; T_{sh,s} \Big|_{z=0^+} = T_{sh,s,in.}, \frac{\partial T_{sh,s}}{\partial z} \Big|_{z=L} = 0; \frac{\partial T_{sh,s}}{\partial r} \Big|_{r=R/2} = \frac{h_{sb}}{\lambda_{r,eff,s}} [T_{sh,b} - T_{sh,s} + \frac{T_{sh,m} + T_{p,m}}{2}] \Big|_{r=0} = 0 \quad (6)$$

2.6 Gaseous bubble's mass transfer in the shell side

Chemical components (i = CH₄, CO₂ and CO) are not permeated because the Pd-based membrane is built to permeate only H₂ of the shell side into the permeation side. Mass balance equations to each component on the gaseous bubble i in the SFBM reformer module's shell side are reported as follows.

- Mass balance of components i on the gaseous bubble in the shell side;

$$\frac{\partial C_{sh,b,i}}{\partial t} = D_{r,eff,b} \frac{1}{r} \frac{\partial}{\partial r} \left(r \frac{\partial C_{sh,b,i}}{\partial r} \right) - u_b \frac{\partial C_{sh,b,i}}{\partial z} + k_{bs,i} \frac{3}{R_p} \frac{(1-\varepsilon_b)}{\varepsilon_b} (C_{sh,b,i} - C_{sh,s,i}) \quad (7)$$

- Initial and boundary conditions for Equation (7) are defined as;

$$C_{sh,b,i} \Big|_{t=0} = C_{sh,b,i,0}; C_{sh,b,i} \Big|_{z=0^+} = C_{sh,b,i,in.}, \frac{\partial C_{sh,b,i}}{\partial z} \Big|_{z=L} = 0; \frac{\partial C_{sh,b,i}}{\partial r} \Big|_{r=R/2} = \frac{k_{bs}}{D_{r,eff,b}} (C_{sh,b,i} - C_{sh,s,i}) \Big|_{r=0} = 0 \quad (8)$$

- Mass balance of H₂ on the shell side;

$$\frac{\partial C_{sh,b,H_2}}{\partial t} = D_{r,eff,H_2} \frac{1}{r} \frac{\partial}{\partial r} \left(r \frac{\partial C_{sh,b,H_2}}{\partial r} \right) - u_b \frac{\partial C_{sh,b,H_2}}{\partial z} + k_{bs,H_2} \frac{3}{R_p} \frac{(1-\varepsilon_b)}{\varepsilon_b} (C_{sh,b,H_2} - C_{sh,s,H_2}) - \frac{\pi}{L} J_{H_2} \quad (9)$$

- Initial and boundary conditions for Equation (9) are defined as;

$$C_{sh,b,H_2} \Big|_{t=0} = C_{sh,b,H_2,0}; C_{sh,b,H_2} \Big|_{z=0^+} = C_{sh,b,H_2,in.}, \frac{\partial C_{sh,b,H_2}}{\partial z} \Big|_{z=L} = 0; \frac{\partial C_{sh,b,H_2}}{\partial r} \Big|_{r=R/2} = \frac{k_{bs}}{D_{r,eff,H_2}} (C_{sh,b,H_2} - C_{sh,s,H_2}) - \frac{\pi}{L} J_{H_2} \Big|_{r=0} = 0 \quad (10)$$

2.7 Solid phase's mass transfer in the shell side

As the solid phase can't permeated through Pd-based membrane, all Chemical components ($i = \text{CH}_4, \text{CO}_2, \text{H}_2$ and CO) are modelled in the solid phase without none mass flow towards the permeation side. Mass balance equations to each component i on the solid phase in the SFBM reformer module's shell side are described as follows.

- Mass balance of each components i on the solid phase in the shell side;

$$\frac{\partial C_{sh,s,i}}{\partial t} = D_{r,eff,s} \frac{1}{r} \frac{\partial}{\partial r} \left(r \frac{\partial C_{sh,s,i}}{\partial r} \right) - u_s \frac{\partial C_{sh,s,i}}{\partial z} - k_{sb,i} \frac{3}{R_p} \frac{(1-\varepsilon_b)}{\varepsilon_b} (C_{sh,b,i} - C_{sh,s,i}) + \rho_s \eta_1 \left[- (r_{\text{CH}_4} + r_{\text{CO}_2}) + 2 (r_{\text{CO}} + r_{\text{H}_2}) \right] \quad (11)$$

- Initial and boundary conditions for Equation (11) are defined as;

$$C_{sh,s,i} \Big|_{t=0} = C_{sh,s,i,0}; C_{sh,s,i} \Big|_{z=0^+} = C_{sh,s,i,in.}; \frac{\partial C_{sh,s,i}}{\partial z} \Big|_{z=L} = 0; \frac{\partial C_{sh,s,i}}{\partial r} \Big|_{r=R/2} = \frac{k_{sb}}{D_{r,eff,s}} (C_{sh,b,i} - C_{sh,s,i}); \frac{\partial C_{sh,s,i}}{\partial r} \Big|_{r=0} = 0 \quad (12)$$

There are complementary equations in Equations (1)-(12). These equations are used to supplement the mathematical model's energy and mass equations and can be found in Equations (13) and (14) below.

$$r_{\text{CH}_4} = -R_{\text{CO}_2}, r_{\text{CO}_2} = -R_{\text{CO}_2}, r_{\text{H}_2} = +2R_{\text{CO}_2}, \text{ and } r_{\text{CO}} = +2R_{\text{CO}_2}; \quad (13)$$

$$J_{\text{H}_2} = \frac{Q_0}{\delta_m} \exp \left(- \frac{E_{\text{H}_2}}{R_u T_{op.}} \right) \left[\left(P_{\text{H}_2}^{sh.} \right)^{0.5} - \left(P_{\text{H}_2}^{per.} \right)^{0.5} \right] \quad (14)$$

2.8 Permeate side

The amount of permeated H_2 depends not only of the membrane properties, but it is also a function of the recovery of H_2 in the permeation side. A mass balance equation was developed for the permeation side as follows.

$$L \frac{dY_{\text{H}_2}^{per}}{dz} = \frac{2\pi LR_m}{F_{\text{CH}_4,0}} J_{\text{H}_2}; F_{\text{H}_2}^{per} \Big|_{z=0^+} = 0, \text{ and } \frac{dY_{\text{H}_2}^{per}}{dz} \Big|_{z=L} = 0 \quad (15)$$

From hydrogen recovery ($Y_{\text{H}_2}^{per.}$), it can be computed the concentration of hydrogen on the permeation side as follows.

$$C_{\text{H}_2}^{per} = \frac{P_{op}^{per.}}{R_u T_{op}^{per.}} Y_{\text{H}_2}^{per} \quad (16)$$

2.9 Model equations numerical solution

The numerical solution of the mathematical model was carried out for a numeric method which ensures numerical

stability (Cruz and Abreu, 2017). The proposed model was solved by the finite volume method (FVM) in together with prescribed initial and boundary conditions to analyze the performance of the SFBM reformer module.

3. Results and Discussion

The mathematical modelling was used to investigate the performance from SFBM reformer module using the solar energy's thermal energy. The physical parameters used to obtain the results are shown in Table 1 as follows.

Table 1: Physical parameters used to obtain the simulation results.

Feed parameters	Values	References
Kinetic constant (k_{CO_2}), kmol/ kg _{cat} .sec	5.775×10^5	Medeiros et al., (2021)
Adsorption constant of CH ₄ (K_{CH_4}), kPa ⁻¹	2.4317×10^{-6}	Dias et al., (2020)
Adsorption constant of CO ₂ (K_{CO_2}), kPa ⁻¹	3.9008×10^{-5}	Dias et al., (2020)
Partial pressure (P_{CH_4}), kPa	5.5664	Ceylan et al., (2017)
Partial pressure (P_{CO_2}), kPa	4.8471	Corumlu et al., (2018)
Inlet bubble Temperature ($T_{sh, b, in}$), K	723	Estimated
Void fraction (ϵ_b), m ³ gas/m ³ reformer	0.92	Abdesslem et al., (2013)
Radial bubble thermal cond. ($\lambda_{r, eff, b}$), $W m^{-1} K^{-1}$	0.126	Kashani et al., (2016)
Bubble cap. in the shell side ($C_{p, sh, b}$), $kJ kg^{-1} K^{-1}$	0.967	Kashani et al., (2016)
Bubble velocity (u_b), $m s^{-1}$	0.721	Dias et al., (2020)
Bubble density ($\rho_{sh, b}$), $kg m^{-3}$	0.0836	Dias et al., (2020)
Bubble -solid heat transfer coef. (h_{bs}), $W m^{-2} s^{-1}$	45.73	Wang et al., (2019)
Interphase specific surface area (A_{bs}), m^{-1}	1700	Wang et al., (2019)
Membrane thickness (δ_w), μm	3.5	Gu et al., (2019)
Solid density ($\rho_{sh, s}$), $kg m^{-3}$	1400	Wang et al., (2019)
Solid cap. in the shell side ($C_{p, sh, s}$), $kJ kg^{-1} K^{-1}$	0.267	Gu et al., (2019)
Solid thermal conductivity ($\lambda_{r, eff, s}$), $W m^{-1} K^{-1}$	0.371	Agrafiotis et al., (2014)
Radial dispersion coef. of bubble ($D_{r, eff, b}$) $m^2 s^{-1}$	2.5×10^{-5}	Taji et al., (2018)
Mass transfer coef. of bubble (k_{bs}), $m s^{-1}$	1.02×10^{-2}	Sun et al., (2017)
Radial dispersion coef. of H ₂ (D_{r, eff, H_2}) $m^2 s^{-1}$	3.47×10^{-6}	Sun et al., (2017)
Radial dispersion coef. of steam ($D_{r, eff, s}$) $m^2 s^{-1}$	5.234×10^{-4}	Gu et al., (2019)

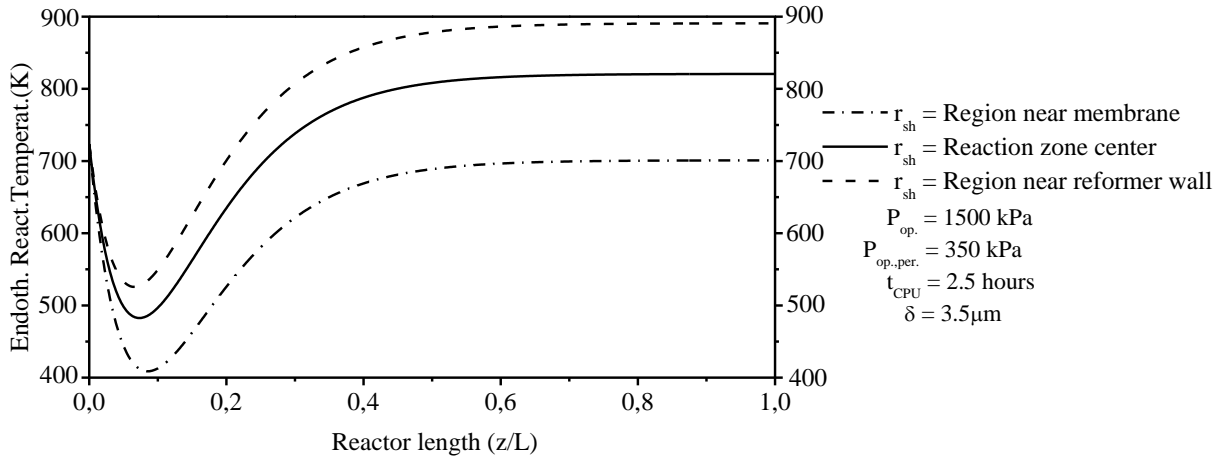
Source: Authors themselves.

3.1 Numerical experiments

Chemical equilibrium is the state in which the forward and backward reaction rates are equal. For this condition, there is no shift in concentrations of the reactants and products. In addition, the thermodynamic equilibrium occurs when a system reaches the chemical and thermal equilibriums. In this study, chemical equilibrium is connected to the mathematical model through the reaction rate's (Eq. (2)) equation. Figure 2 shows the endothermic reaction's temperature profiles in the shell side

with particles of β -SiC open-cell foam to three different radial positions.

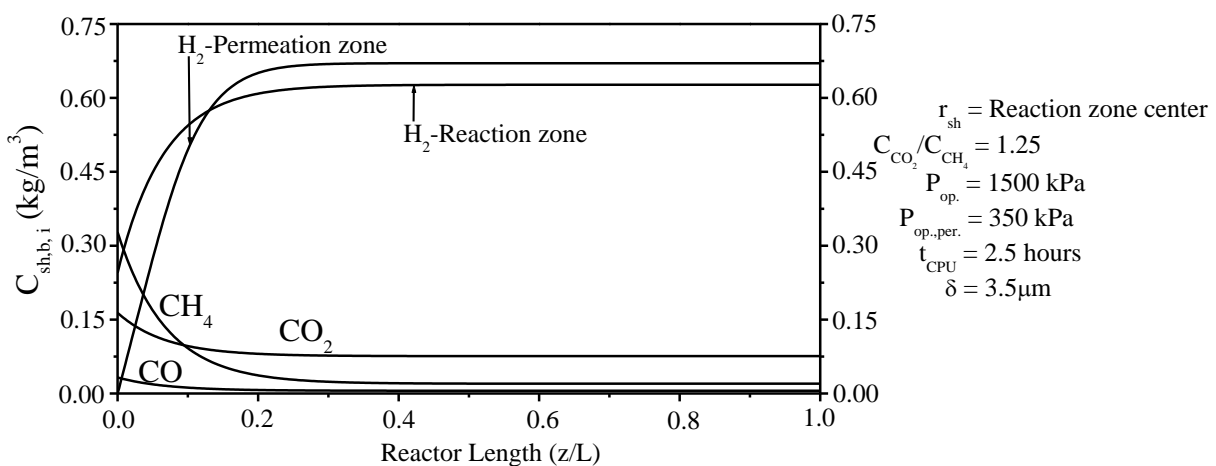
Figure 2. Temperature profiles versus reformer length for three different radial positions to an average effective radial conductivity ($\lambda_{r,eff,s} = 0.159 \text{ w m}^{-1} \text{ K}^{-1}$).



Source: Authors themselves.

Because of the endothermic nature of the reforming reaction, heat is supplied into by means of external heating. Therefore, the SFBM reformer' reaction zone and catalyst particles are exposed to significant temperature gradients. Figure 2 describes a significant decrease of the reaction temperature towards to Pd-based membrane due to thermodynamic equilibrium's shift.

Figure 3. Mole concentration of the components versus reformer length at averaged radial position to an average effective radial conductivity ($\lambda_{r,eff,s} = 0.159 \text{ w m}^{-1} \text{ K}^{-1}$).



Source: Authors themselves.

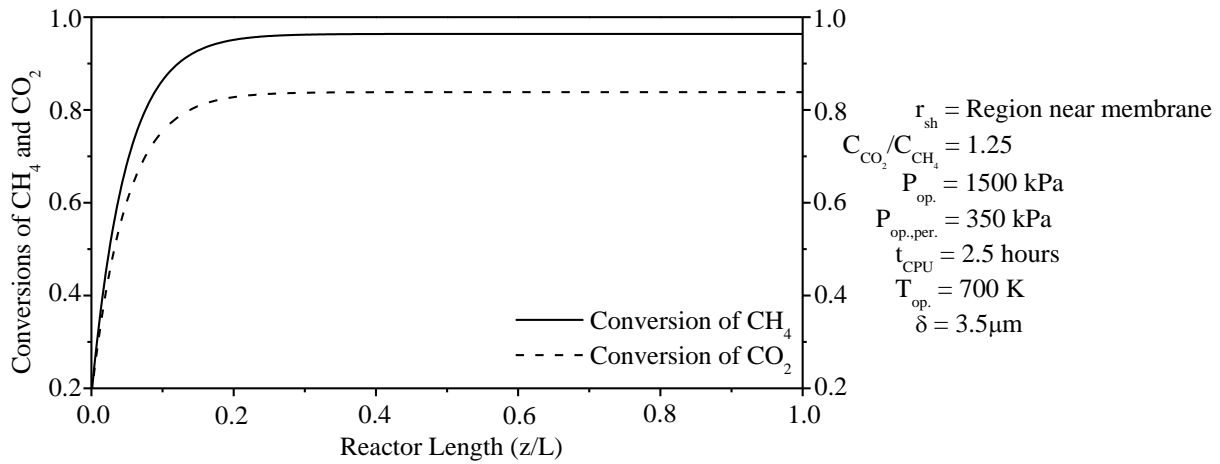
Figure 3 shows that the distribution of the gaseous products can reach to stable levels instantly after introducing the initial values. As it can be observed in Figure 3, the reactant mole concentration (CH_4 and CO_2) distributions decrease sharply along SFBM reformer bed and therefore, reactant mole concentration distributions have small fluctuation along SFBM reformer bed up to the gas outlet surface. The mole concentration of H_2 (reaction and permeation regions) increases

remarkably at the near gas inlet surface region and reaches their maximum values at the gas outlet surface.

After reporting the temperature profiles at the radial positions in the shell side, it is possible to compute the conversions of CH₄ and CO₂ at the region near membrane.

$$X_{CH_4} = 1 - \frac{C_{sh,s,CH_4}}{C_{sh,s,CH_4,in}}; X_{CO_2} = 1 - \frac{C_{sh,s,CO_2}}{C_{sh,s,CO_2,in}} \quad (17)$$

Figure 4. Conversion of CH₄ and CO₂ versus reformer length at near membrane radial position to an average effective radial conductivity ($\lambda_{r,eff,s} = 0.159 \text{ w m}^{-1} \text{ K}^{-1}$).



Source: Authors themselves.

The major advantage of dry reforming of CH₄ in membrane reactors is the conversion progress of by the hydrogen removal through the selective membrane, but the conversion of reactants (CH₄ and CO₂) is usually limited by the thermodynamic equilibrium due to equilibrium-limited reversible kinetics rate. Figure 4 reports a comparison between the conversion of CH₄ and conversion of CO₂ along SFBM reformer length.

4. Conclusion

This work has been focused on the physical-mathematical modelling of the heat and mass transfer for a SFBM reformer module. An analysis to report the performance of the reaction temperature, production of H₂, and conversion of CH₄ and CO₂ is carried out and can be summarized the following conclusions:

1. Pd-based membrane has a significant effect on the thermodynamic equilibrium's shift and thus, the SFBM reformer operates on lower temperature in comparison to a conventional reformer;
2. The amount of H₂ in the permeation zone is higher in comparison with the quantity of H₂ in the reaction zone;
3. The overall conversions of reactants have reached the maximum values of 96.17 % (CH₄) and 83.21% (CO₂).

For future work, the developed model's validation can be investigated from experimental data. Open-cell foams are potential materials to enhance thermal energy storage and therefore, it is interesting to study new reforming processes of CH₄ applying open-cell foams.

Acknowledgments

The authors are grateful to University of Pernambuco for the financial support given (Project 127/2019).

References

- Abdesslem, J., Khalifa, S., Abdelaziz, N., & Abdallah, M. (2013). Radiative properties effects on unsteady natural convection inside a saturated porous medium. Application for porous heat exchangers. *Energy*, 61, 224-233. 10.1016/j.energy.2013.09.015.
- Agrafiotis, C., Storch, H. V., Roeb, M., & Sattler, C. (2014). Solar thermal reforming of methane feedstocks for hydrogen and syngas production-A review. *Renew Sust Energy Reviews*, 29, 656-682. 10.1016/j.rser.2013.08.050.
- Ceylan, I., Gurel, A. E., & Ergun, A. (2017). The mathematical modeling of concentrated photovoltaic module temperature. *Int J Hydrogen Energy*, 42, 19641-19653. 10.1016/j.ijhydene.2017.06.004.
- Chein, R. Y., Hsu, W. H. and Yu, & C. T. (2017). Parametric study of catalytic dry reforming of methane for syngas production at elevated pressures. *Int J Hydrogen Energy*, 42, 14485-14500. 10.1016/j.ijhydene.2017.04.110.
- Chen, X., Wang, F., Yan X., Han, Y., Chen Z. & Jie Z. (2018). Thermochemical performance of solar driven CO₂ reforming of methane in volumetric reactor with gradual foam structure. *Energy*, 151, 545-555. 10.1016/j.energy.2018.03.086.
- Cruz, B. M. & Silva, J. D. (2017). A two-dimensional mathematical model for the catalytic steam reforming of methane in both conventional fixed-bed and fixed-bed membrane reactors for the Production of hydrogen. *Int J Hydrogen Energy*, 42, 23670-23690. 10.1016/j.ijhydene.2017.03.019.
- Corumlu, V., Ozsoy, A., & Ozturk, M. (2018). Thermodynamic studies of a novel heat pipe evacuated tube solar collectors based integrated process for hydrogen production. *Int J Hydrogen Energy*, 43, 1060-1070. 10.1016/j.ijhydene.2017.10.107.
- Dias, V. F., & Silva, J. D. (2020). Mathematical modelling of the solar-driven steam reforming of methanol for a solar thermochemical micro - fluidized bed reformer: thermal performance and thermochemical conversion. *J Braz Soc Mech Sci Eng*, 42, 447. 10.1007/s40430-020-02529-6.
- Gu, R., Ding, J., Wang, Y., Yuan, Q., Wang, W., & Lu, J. (2019). Heat transfer and storage performance of steam methane reforming in tubular reactor with focused solar simulator. *Appl Energy*, 234, 789-801. 10.1016/j.apenergy.2018.10.072.
- Jin, J., Wei, X., Liu, M., Yu, Y., Li, W., Kong, H. & Hao, Y., (2018). A solar methane reforming reactor design with enhanced efficiency. *Applied Energy*, 226, 797-807. 10.1016/j.apenergy.2018.04.098.
- Kashani, M. N., Elekaei, H., Zivkovic, V., Zhang, H., & Biggs, M. J. (2016). Explicit numerical simulation-based study of the hydrodynamics of micro-packed beds. *Chem Eng Sci*, 145, 71-79. 10.1016/j.ces.2016.02.003.
- Medeiros, J. P. F., Dias, V. F., Silva, J. M. & Silva, J. D. (2021). Thermochemical performance analysis of the steam reforming of methane in a fixed bed membrane reformer: A modelling and simulation study. *Membranes*, 11, 6, 1-26. 10.3390/membranes11010006.
- Nagy, E., (2010). Coupled effect of the membrane properties and concentration polarization in pervaporation: Unified mass transport model. *Separation and Purification Technology*, 73, 194-201. 10.1016/j.seppur.2010.03.025.
- Reis, M. C., Sphaier, L. A., Alves, L. S. B. & Cotta, R. M. (2018). Approximate analytical methodology for calculating friction factors in flow through polygonal cross section ducts. *J Braz Soc Mech Sci Eng*, 40, 76. 10.1007/s40430-018-1019-6.
- Silva, J. D. & Abreu, C. A. M. (2016). Modelling and simulation in conventional fixed-bed and fixed-bed membrane reactors for the steam reforming of methane. *Int J Hydrogen Energy*, 41, 11660-11674. 10.1016/j.ijhydene.2016.01.083.
- Silva J, M., Dias, V. F., & Silva, J. D. (2021). Mathematical modelling of the residence time distribution of CO₂ tracer in a three-phase micro-packed bed reactor: An experimental analysis. *Research, Society Develop.*, 10, 9, e23210917425. 10.33448/rsd-v10i9.17425
- Sun Y, Jia Z, Yang G, Zhang L, & Sun Z (2017). Fischer-Tropsch synthesis using iron based catalyst in a microchannel reactor: Performance evaluation and kinetic modeling. *Int J Hydrogen Energy*, 42, 29222-29235. 10.1016/j.ijhydene.2017.10.022.
- Taji M, Farsi M, & Keshavarz P (2018). Real time optimization of steam reforming of methane in an industrial hydrogen plant. *Int J Hydrogen Energy*, 43, 13110-13121. 10.1016/j.ijhydene.2018.05.094.
- Villafán-Vidales H. I., Arancibia-Bulnes C. A., Riveros-Rosas D., Romero-Paredes H., & Estrada C. A. (2017). An overview of the solar thermochemical processes for hydrogen and syngas production: Reactors and facilities. *Ren Sust Energy Reviews*, 75, 894-908. 10.1016/j.rser.2016.11.070.
- Wang H, Liu M, Kong H, & Hao Y (2019). Thermodynamic analysis on mid/low temperature solar methane steam reforming with hydrogen permeation membrane reactors. *Appl Therm Eng*, 152, 925-936. 10.1016/j.applthermaleng.2018.03.030.